Supplementary Materials

Amanda Wild, Jean Braun, Alex Whittaker, and Sebastien Castelltort

February 6, 2024

1 Figures

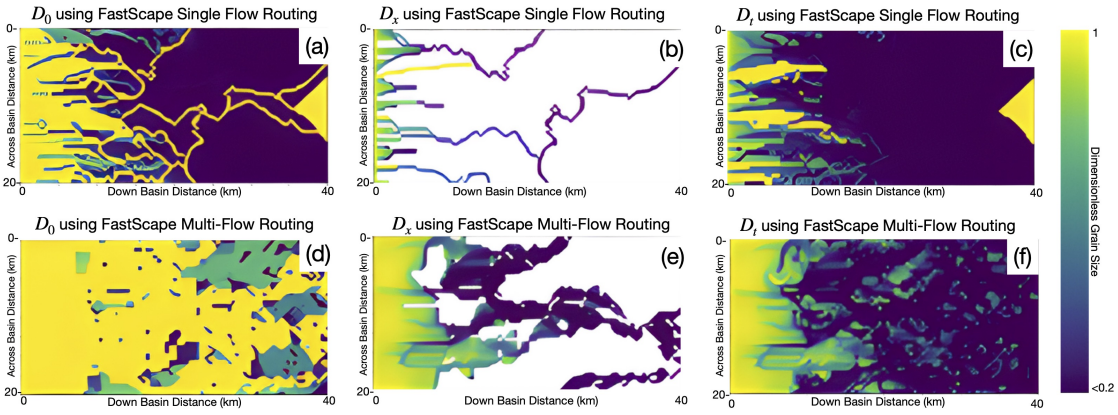

Figure 1: *using the same constant inputs at steady-state, basin panels A-C show the FastScape single flow routing and panels D-F display the multi-flow routing for grain size D_0, D_x, and D_t grids (from left to right respectively). The D_0 grid shows the source grain size propagated through the drainage routing of a given time step based on 1) the sediment deposited during previous time steps (previous D_t grid) or 2) , if the solution erodes or reaches (under-filled basin without ample sediment) bedrock (eg: end of the basin), then the grain size is set to the incoming grain size from the source or bedrock (1 when dimensionless). D_x is the grain size fining that occurred in the channels of a given instantaneous time step (in this case the final model time step at steady-state). D_t is the surface grain size updated after each time step by the drainage/ grain sizes deposited and where the exposed bedrock is shown with a grain size of 1. The FastScape multi-flow routing package was used for all other figures and analyses within this work. However, the single flow routing package is shown for the purpose of contrast and to highlight for future model users that the computation of grain size is also possible with the single flow routing of FastScape.*

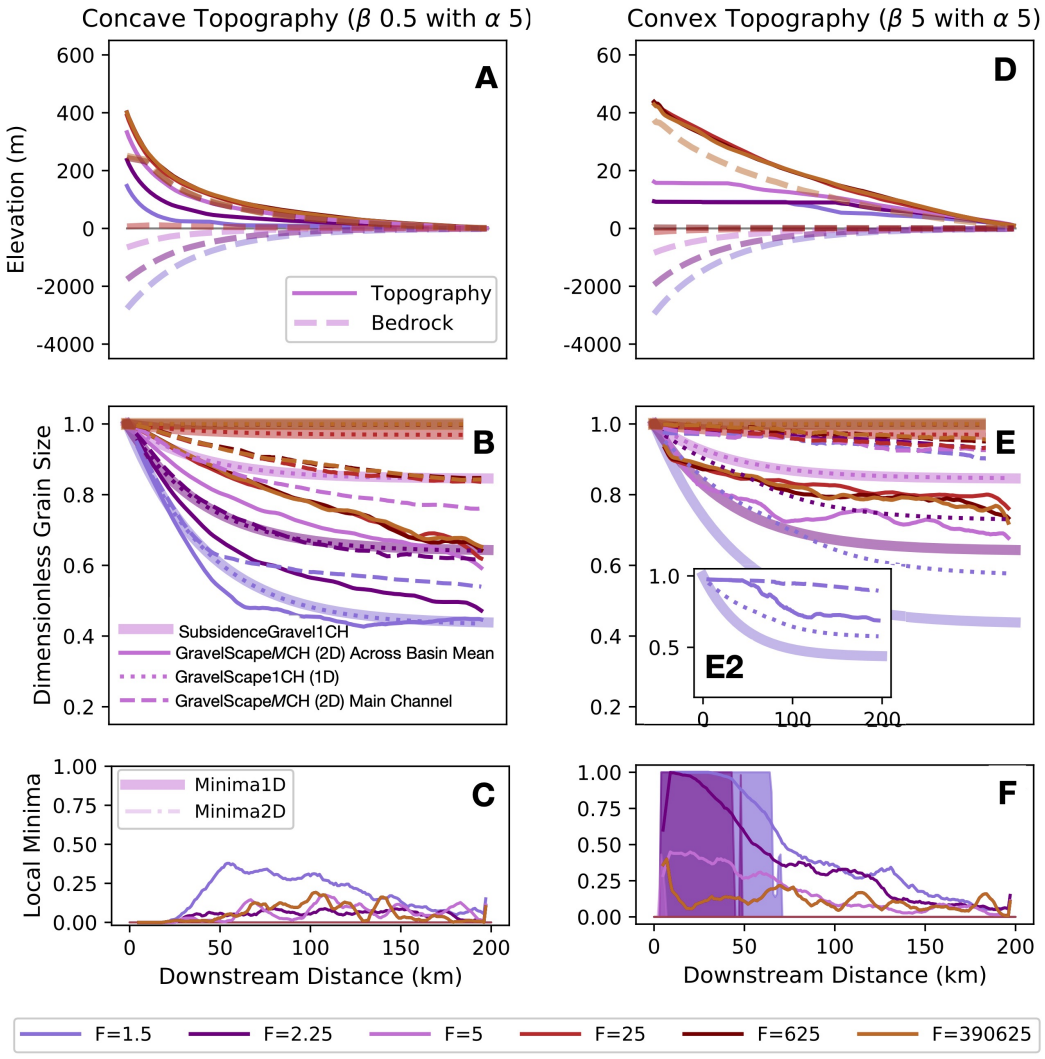

Figure 2: *shows an alternate initial single vs multi-channel validation very similar to that presented in the main text, but including the grain size trends in the main channel and averaged across the basin with substantial local minima impacting the drainage routing and impacting the grain size fining. Especially in panel E2 (the first 75km of the basin are a local minima), one can see how the channel grain size in single (1D) channel or multi-channel (2D) are both much coarser than the theoretical solution due to the drainage being forced directly to the model outlet. Panels A and D show the steady-state average basin topography (solid) and underlying bedrock subsidence (dash-dot). Subsets labelled B and E show the grain size fining from the SubsidenceGravel1CH (thickets lines with opacity), GravelScape1CH (dotted lines) (1D), and GravelScapeMCH (thin-solid and long-dash lines) (2D) solutions. Subset images 3 show the frequency of local minima occurring within the basin.*

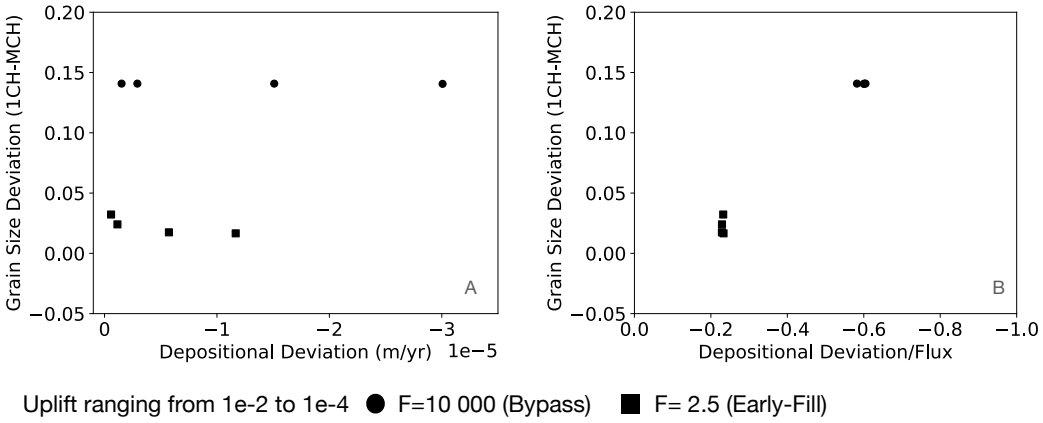

Figure 3: *Four values of varying uplift rates/sediment flux, tested with varying subsidence rates to produce high (circles) and low (squares) F, produced higher deposition deviation with higher flux without impacting grain size deviation (panel A). Panel B demonstrates that when changing sediment flux (through varying uplift rates in panel A), one must divide the depositional divergence by the flux in order to get the same correlation trend with grain size divergence that vary with F (right side) as presented in main paper. Models were run to steady-state using different uplift rates to control the flux.*

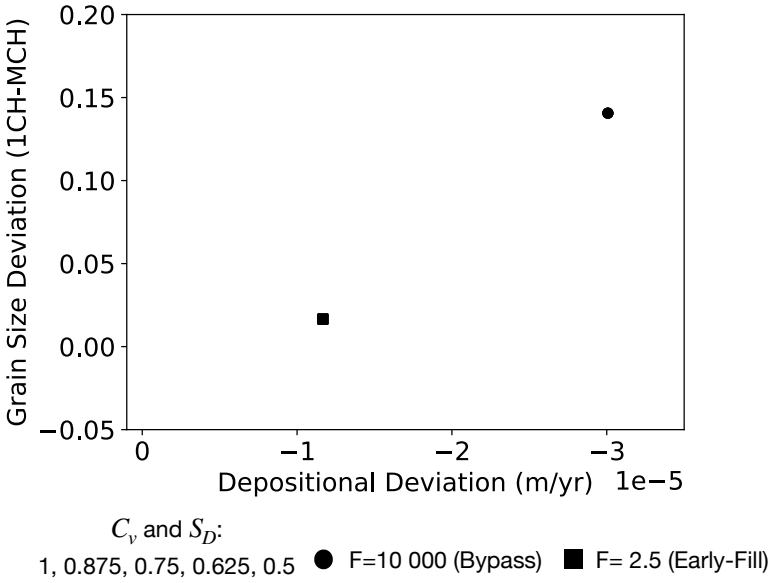

Figure 4: *There is no change in depositional or grain size divergence with varying grain size CV and SD. Four values of CV and SD were tested for each F (high (circles) and low (square)) set-ups. They all were the same and this only appear as a single value depending on F.*

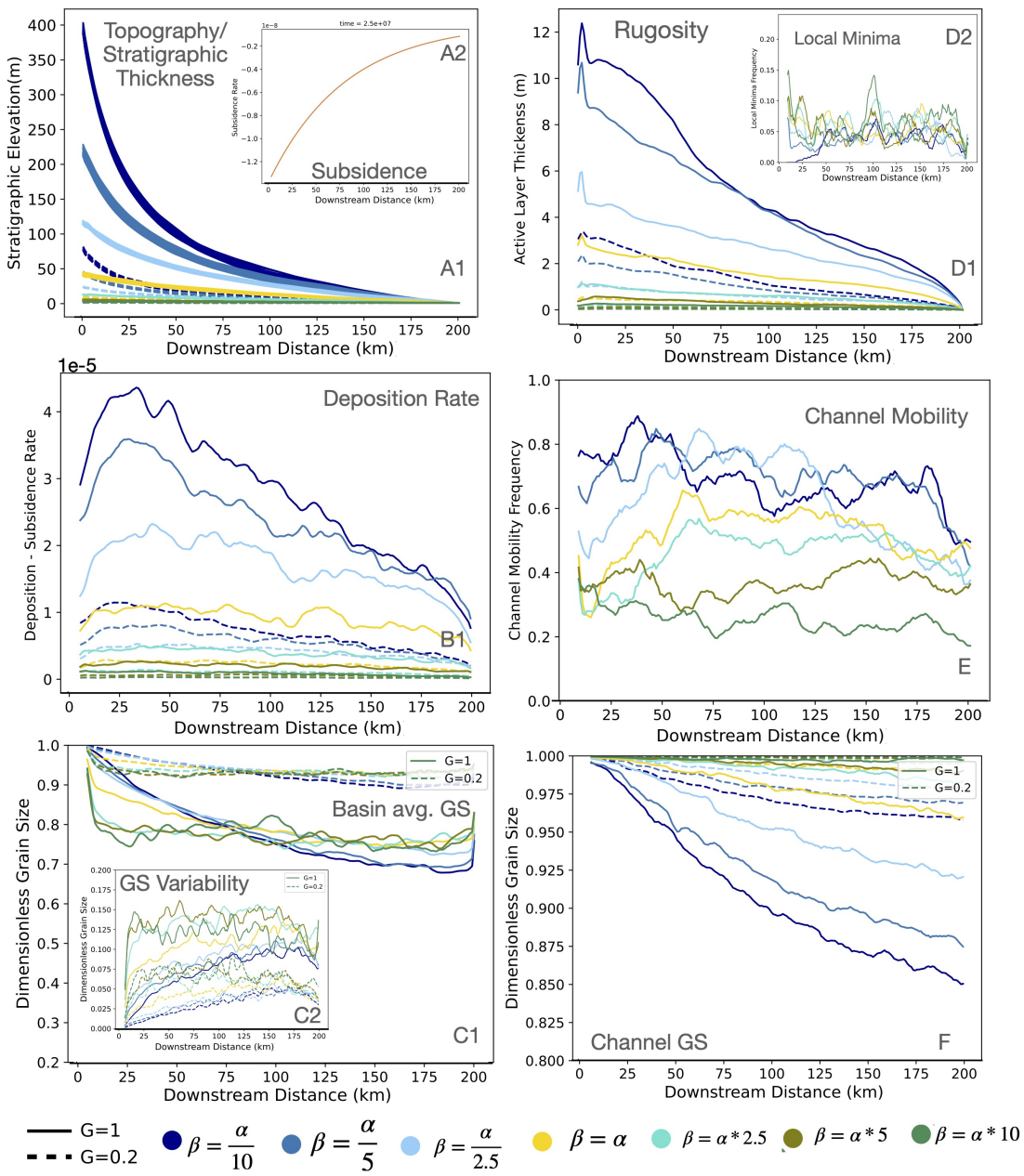

Figure 5: *Autogenic parameters within the landscape evolution mode with downstream distance preserved while changing beta through orogen precipitation at steady-state. Blue lines represent low upstream discharge, low beta, and steep-concave topography while yellow-green represents high upstream discharge, high beta, and flat-convex topography. We show the steady-state downstream (x) progression of across basin (y) average: topography/stratigraphic thickness (A1) with underlying subsidence (A2) under high bypass (F¿100); active layer thickness (D1) and local minima frequency (D2 where all solutions are under 25 percent); depositional divergence from subsidence rate (B1); channel mobility (E); basin average grain size fining (C1) with variation in grain size over time and space (C2); and grain size within the main channel (F). Grain size is shown dimensionless grain size units with a source of 1. Solid lines represent a G=1 and dashed show the G=0.2 solution. All solutions are for a high bypass (F¿100) topography to show the variation in autogenic parameters with x preserved under highest potential autogenic conditions identified within the main text.*

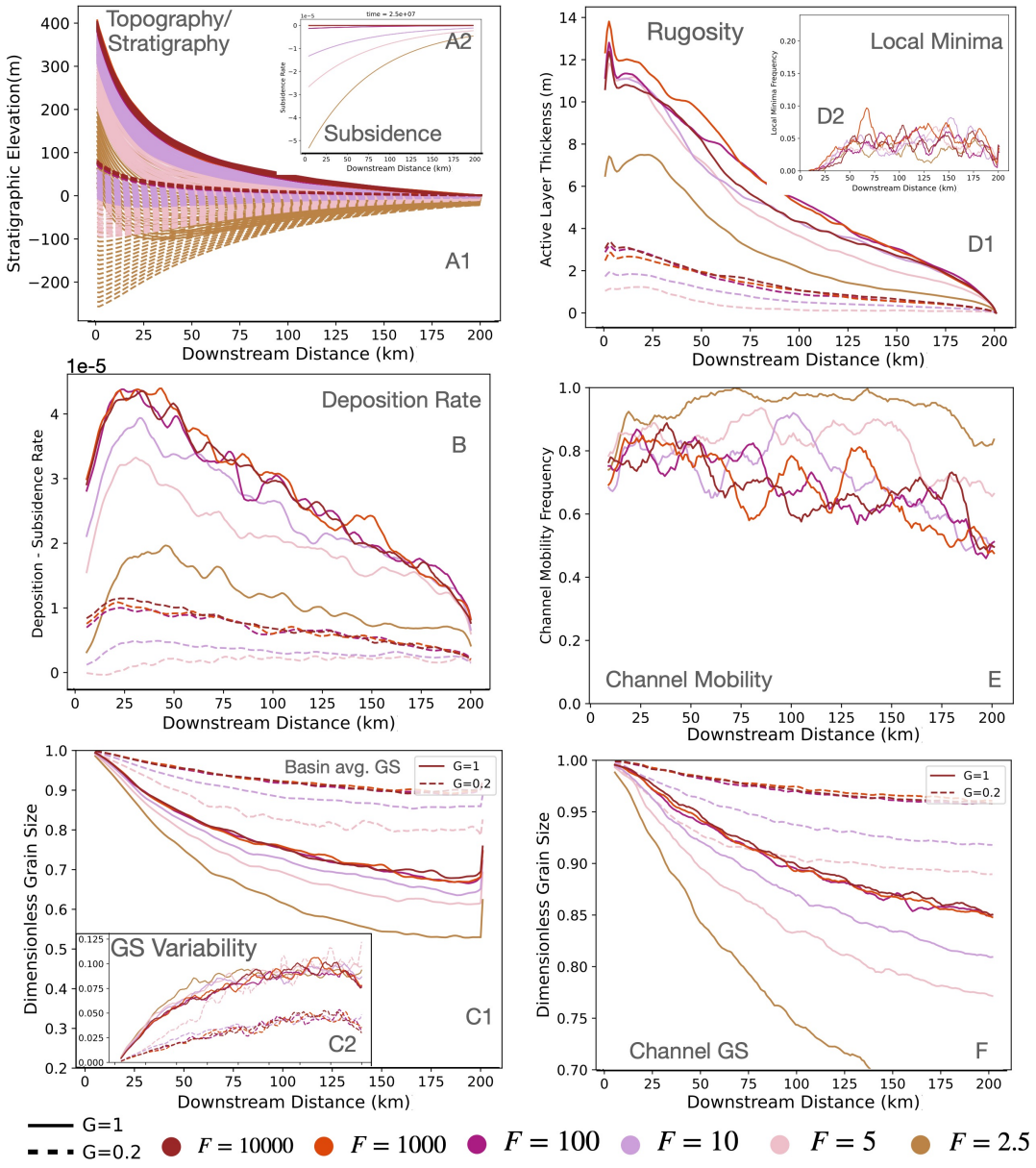

Figure 6: *Autogenic parameters within the landscape evolution mode with downstream distance preserved while changing F through underlying subsidence within the basin at steday-state. Gold to pink lines represent low to mixed filling conditions with greater subsidence and lower F. Dark red-orange represent high bypass conditions with little underlying subisdence. We show the steady-state downstream (x) progression of across basin (y) average: topography/stratigraphic thickness (A1) with underlying subsidence (A2); active layer thickness (D1) and local minima frequency (D2 where all solutions are under 25 percent); depositional divergence from subsidence rate (B1); channel mobility (E); basin average grain size fining (C1) with variation in grain size over time and space (C2); and grain size within the main channel (F). Grain size is shown dimensionless grain size units with a source of 1. Solid lines represent a G=1 and dashed show the G=0.2 solution. All solutions are for a low beta (beta=alpha/10) to show the variation in autogenic parameters with x preserved under highest potential autogenic conditions identified within the main text.*

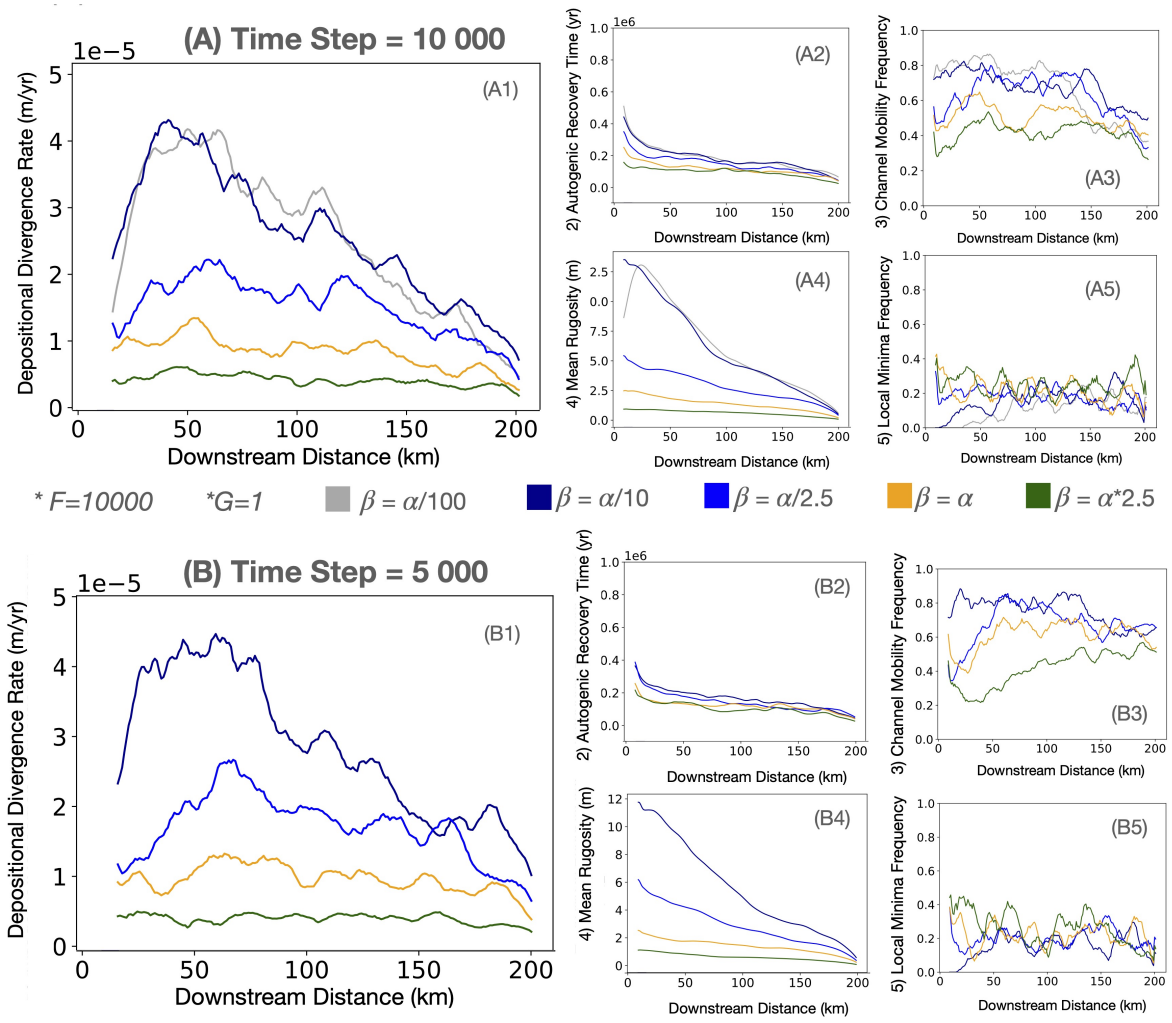

Figure 7: *Explores the impact of changing time step (10000 vs 5000 yrs) on various autogenic paramters with downstream distance preserved for a constant, high bypass solution (high* $F = 10000$*) with a G=1 allowing for autogenic dynamics while varying topography through* β *(green (low-convex) to grey (steep-concave)). Results are averaged over 5Myrs at steady-state after running the model for 25Myrs. In the main text, depositional divergence was noted as the strongest correlated parameter to autogenic grain size divergence. With changing time step, although the exact downstream trend slightly differs, the depositional divergence is comparable. The impact of changing additional autogenic parameters (that had a weaker correlation to grain size fining/divergence) such as recovery time, channel mobility, local minima and rugosity are shown in the subsequent panels where rugosity and channel mobility were more sensitive to the changing time step.*